Electrochemical and Solid-State Letters, **9** (9) H85-H87 (2006)
1099-0062/2006/9(9)/H85/3/$20.00 © The Electrochemical Society

Single-Wall Carbon Nanotube-Based pH Sensor Fabricated by the Spray Method

Jae-Hong Kwon,[a] Kyong-Soo Lee,[b] Yun-Hi Lee,[b] and Byeong-Kwon Ju[a,z]

[a]*Display and Nanosystem Laboratory, College of Engineering, and* [b]*Department of Physics, Korea University, Seoul 136-701, Korea*

The concentration of the hydroxyl ion is a critical parameter which must be measured for monitoring the condition of aqueous biological species or for predicting the path of chemical reactions. This paper describes a method for fabricating a simple and fast response pH sensor composed of single-wall carbon nanotubes (SWCNTs) using a spray. Such a CNT-based sensor shows amperometric response in buffer solution at different hydroxyl ion concentrations. Our results suggest that sprayed CNT sensors can be used as chemical sensors and biosensors in future large-scale throughput devices.
 [DOI: 10.1149/1.2217131]

Manuscript submitted January 12, 2006; revised manuscript received May 19, 2006. Available electronically June 27, 2006.

The recent advancement in carbon nanotube (CNT) nanotechnologies has provided viable solutions.[1-3] CNTs with their well-defined nanoscale dimensions and unique molecular structure can be used as bridges linking biomolecules to macro/micro-solid-state devices so that bioevent information can be transduced into measurable signals.[3] Both the solubility of many chemicals or biomolecules in solution and the speed or rate of (bio)chemical reactions are dependent on pH. To optimize the desired reaction and to prevent unwanted reactions, controlling the pH of solutions is also very important. Due to the extreme sensitivity of CNTs, the detection of chemicals, or even a small bio-molecule, will be realized.[4] Because the biological sensing should be performed in an aqueous phase, the effect of the change in the concentrations of hydrogen ions (H^+) and hydroxyl ions (OH^-) on the electrical properties of CNTs should adequately be investigated in this field of study. Because of the high demand for the chemical characteristics monitoring of a substance, different groups have extensively studied the single-semiconductor CNT[4] or random networks of single-wall (SW)-CNTs,[5] which are used to construct sensing materials, in pH-sensitive field-effect transistors (pH-FETs).[4] However, these techniques, device fabrication methods yielding CNTs growth, have complex and limited controllability, and therefore are slow and expensive, not applicable for mass-production of devices, because manipulating individual carbon nanotube[6,7] and random dispersion of suspended carbon nanotubes onto prepatterned electrodes are fabricated by lithographically patterning a catalyst (as CNT nucleation sites) on electrodes.[8,9] In contrast, sprayed, bundled SWCNTs are easily produced either by direct growth on a catalyzed substrate or by deposition onto an arbitrary substrate from a solution of suspended SWCNTs. To our knowledge, sprayed CNT-based devices have not been used as pH sensors, although sprayed CNT-based applications were used.[10,11] This work aims to develop a simple mass-fabrication method for the sprayed SWCNT-based pH sensor.

Experimental

The SWCNT powder (purchased from Iljin Nanotech Co., Ltd.) had grains of 1–1.2 nm in average diameter, 5–20 μm length, and ~90% purity (prepared by arc-discharge process). Prior to the SWCNT manipulation, 40 mg of the sample was ultrasonically dispersed in 100 mL ethanol solution and the resulting solution was diluted to 0.4 mg/mL or lower concentration for later use.

The fabrication process of the sprayed SWCNT-based pH sensor is shown in Fig. 1. As seen in the fabrication process, SiO_2 is first deposited on the silicon substrate to prevent conduction of the Cr electrode with the substrate. Then, photoresist (AZ 7220 photoresist, Clariant Industries, Ltd.) is spun-on and patterned on the substrate. This photoresist layer can be used as a sacrificial layer for particular applications of the sensors. Afterward, Cr is deposited on the top of the bottom patterned layer, and the sacrificial layer is released using an etchant (AZ REMOVER 700, Clariant industries Ltd.) to serve as mechanical microbridges that suspend the SWCNT sensor across the Cr electrodes. This gap distance between electrodes is 4 μm. Based on the technique for CNT manipulation presented in the previous paragraph, the bundled SWCNT is manipulated and connected across the microelectrode of each sensor. Finally, bundled SWCNT is dispersed on the shadow mask by using a spray (LiPO, Functional Materials Institute). To describe the pH response of the bundled SWCNT, 0.5 μL of pH buffer solution (Tokyo Kasei Kogyo Co., Ltd.) and micropipette are used (Eppendorf Co., Eppendorf Research Pipettes). Real-time current is measured by using a calibrated Keithley (Keithley Instruments, Inc., 4200 SCS) at room temperature. The surface geometry of bundled SWCNT is observed by field-emission-scanning electron microscope (FESEM) Hitachi S-4300 unit.

Results and Discussion

Figure 2 shows the schematic diagram of the SWCNT-based sensor presented in this work. The sensing area of the SWCNT with the

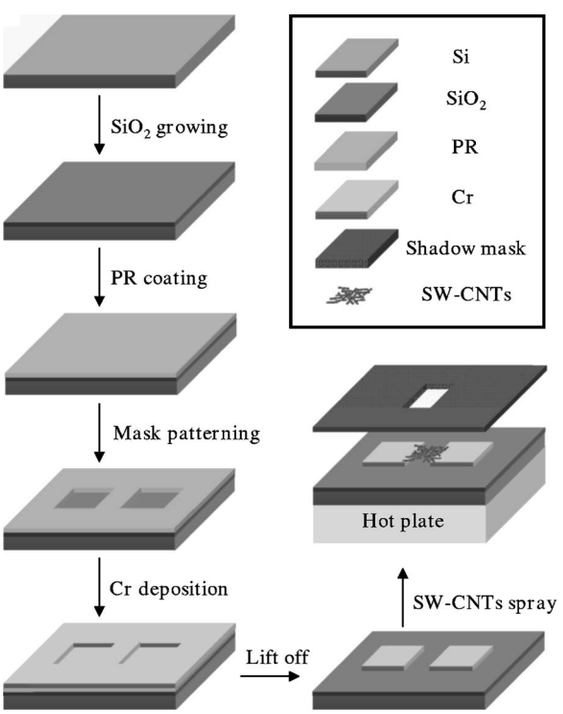

Figure 1. Fabrication process flow for the sprayed SWCNT-based sensor.

[z] E-mail: bkju@korea.ac.kr

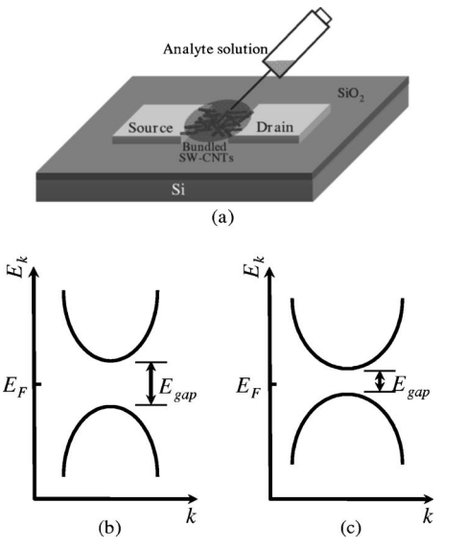

Figure 2. Schematic of mechanism for the SWCNT pH sensor, (a) OH group is attached on the sensing area of the SWCNTs. (b) *E–k* diagram for zigzag (10 × 0) SWCNT. (c) *E–k* diagram for SWCNT + OH system. Typical *E–k* diagram for the hypothetical one-dimensional solid for wavevector *k* values is shown, respectively, for b–c.

OH group and OH^- attached on the wall of the SWCNT, *E–k* diagram for zigzag (10 × 0) SWCNT without OH^-, and *E–k* diagram for SWCNT with absorbed OH^- are shown in Fig. 2a-c, respectively. When the OH group is introduced to the tube wall, a peak in the dense of state (DOS) arises at the Fermi level (E_F), and the energy gap (E_{gap}) is significantly reduced, as shown in Fig. 2c. This result is due to the interaction between the tube and the oxygen because the p_x orbital of oxygen and the p orbital of one carbon atom form a bond, which splits the degenerate levels in the pure SWCNT. The OH group possesses an unpaired electron, which actively participates in hybridization near the carbon atom when the OH group is attached to the tube. OH group can form an acceptor level and enhance the conductivity of the CNT. That is, the OH group can be a good acceptor for hole doping.[12] Also, in light of CNT redox chemistry, we propose that the previously reported bleaching of the CNT absorbance spectrum upon lowering the pH is most likely a consequence of the oxidation of the nanotubes by oxygen.[13] These results demonstrate facile oxidation and reduction of CNTs, provide a way to quantify the population of valence electrons, and point to possible applications of CNT in the catalysis of redox reactions. In other words, the reduction potential of CNT increases with increasing E_{gap}, and it is expected that a gradual oxidation by oxygen from smaller to larger E_{gap} tubes takes place as the pH drops.[14] This explains the observed trend of the pH effect.

The reactive binding group, the hydroxyl ion, may play a key role in electron acceptance. CNTs may facilitate electron transfer between a donor and an acceptor by increasing the reaction cross section. That is, the conductivity of CNT increases with the appearance of OH group and SWCNT with OH^- induces stretching bands corresponding with the reduction process. The mechanisms of pH sensing for CNT have been presented from other groups.[15,16]

Figure 3 shows an FESEM image of random networks of SWCNTs in the region between the source-drain electrodes. This gap distance of sensing area is between 5 and 6 μm. The vine-like morphology of SWCNTs allows foreign molecules (whether from a gas or a liquid) to readily access nanotubes throughout the entire sensing material via micro- to nanometer-sized vine between these bundles. We experimentally found that the resistances of the SWCNTs at room temperature typically range from several kilohms to several hundred kilohms, depending on the lattice geometries of

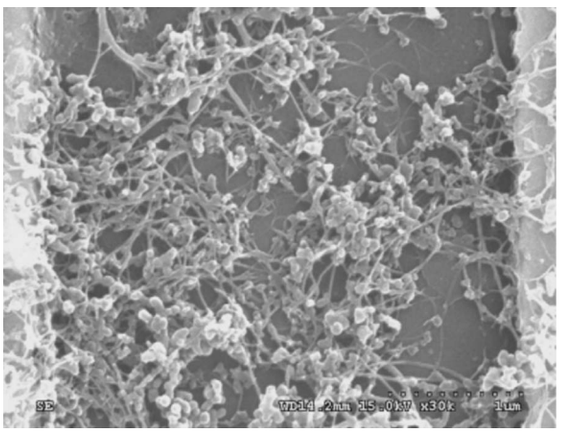

Figure 3. FESEM image of SWCNTs bridging two metal electrode pads on a substrate consisting of randomly overlapped bundles for molecular absorption.

the SWCNTs during the spray process and the weak side-bonding between bundled SWCNTs and electrodes created by van der Waals interaction.[17] Therefore, different SWCNTs exhibited different conductivities.

Figure 4 shows that the conductance of SWCNTs could be substantially increased or decreased upon their exposure to pH buffer solutions, such as that shown in the inset. For monitoring the conductance change of SWCNTs, 0.5 μL of buffer solution at pH 4 and 10 is placed on top of the sensing area. In other words, high and low concentrations of hydroxyl ions are measured. Figure 4 shows that conductance increases with hydroxyl ions concentrations. The changes in conductivity ($\Delta I/\Delta V$, slope) also depend on the pH value. Due to hydroxyl ions attached on the wall of the SWCNTs, pH buffer solutions can decrease or increase the conductance, depending on whether the E_F of the metal + SWCNTs contact was placed at a higher or lower energy level than that of bare SWCNTs.[18]

Figure 5 shows the real-time current measurement of the drain current as a function of time for a SWCNT-based sensor. The response was recorded by adding increasing concentrations of hydroxyl ions into the SWCNTs from 10^{-3} to 10^{-15} M. The device was exposed to rabbit hydroxyl ions (1 mM) as control for selectivity (1st arrow). Lack of a significant signal after this addition indicated successful blocking of structurally similar but nonspecific hydroxyl ion concentrations. Next, 10 μM was added, where upon a signal

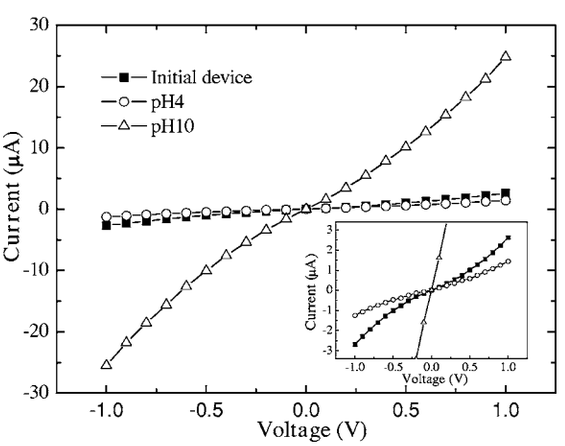

Figure 4. Current–Voltage characteristics of bundled SWCNT sensors at two different pH buffer solutions.

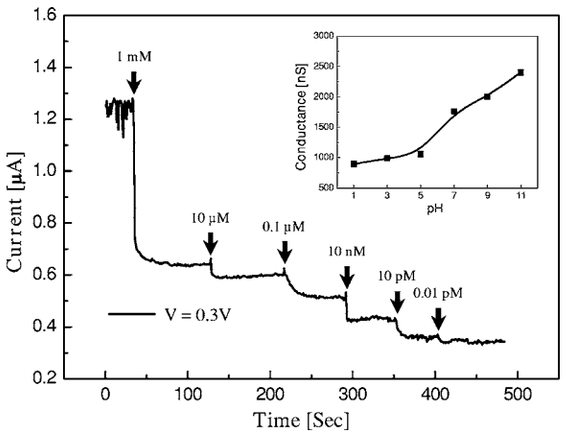

Figure 5. Typical amperometric response of random networks of SWCNTs at room temperature upon the addition of increasing concentrations of hydroxyl ions. (Inset) Conductance resulting from increasing concentrations of hydroxyl ions.

change was observed, indicating a successful binding of the OH group to the device preadsorbed with OH^- (2nd arrow). OH^- at the 0.1 μM concentration level yielded an additional, relatively proportionate response (3rd arrow). Other responses were recorded by adding increasing concentrations such as 10 nM, 10 pM, and 0.01 pM, respectively, for 4th–6th arrow. In addition, taking into consideration the time scale of the still-discrete changes in amperometric response after 6th arrow, this result is associated with binding/unbinding relatively low-containing analyte in sensing area. Although response properties of sprayed SWCNT-based sensor for 0.01 pM are degenerated, it can be seen that the response at ultrasmall concentration is very fast as pH sensor. Also, the inset to Fig. 5 shows the increase of conductance with increase of hydroxyl ion concentrations. These data indicated that the pH value is responsible for the measured increase in conductance from 1 to 11. The conductance change is small at low pH range (1–5) but large at high pH range (7–11). Notably, these pH measurements on SWCNTs are in excellent agreement with previous measurements of the pH-dependent surface charge density derived from carbon.[19] Our work shows that carbon nanotubes are very sensitive to ambient condition: charge transfer due to molecular adsorption to the CNT can drastically change the conductance of the device. Namely, the increase in conductance with increase of pH is consistent with the increase of OH group-doping concentration. Thus, sprayed CNT-based sensors are capable of highly sensitive and selective real-time detection of chemical molecules and biomolecules. The OH group does not etch the tube because of oxidization. Also, the OH doping can be an effective mechanism for modifying the electronic properties of SWCNTs to make SWCNTs a possible candidate for chemical and biosensors.

Conclusions

The present work leads to two important directions of study. First, the fabrication method of a novel pH sensor applicable for mass-production process was presented. Our experimental process flow for pH sensor fabricated by a spray can be divided into three parts: (*i*) fabrication of microelectrodes, (*ii*) sensing material fabrication; and (*iii*) experimental testing. Second, the device is measured by depositing ultrasmall concentrations of hydroxyl ion, and its electrical conductance is monitored while hydroxyl ions are added to the solution. These results show that our technique can be further optimized for increased sensitivity and selectivity for aqueous-phase sensing. Thus, we expect this fabrication method to be very a promising technique for CNT-based sensor applications.

Acknowledgments

The project is funded by the Leading Edge R&D Program of the (Institute for Information Technology Advancement) in the Ministry of Information and Communication.

Korea University assisted in meeting the publication costs of this article.

References

1. S. B. Sinnott and R. Andrews, *Crit. Rev. Solid State Mater. Sci.*, **26**, 145 (2001).
2. S. K. Smart, A. J. Cassady, G. Q. Lu, and D. J. Martin, *Carbon*, In press. Available online Nov 22, 2005.
3. W. Joseph, *Electroanalysis*, **17**, 7 (2004).
4. K. Besteman, J.-O. Lee, F. G. M. Wiertz, H. A. Heering, and C. Dekker, *Nano Lett.*, **3**, 727 (2003).
5. Q. Fu and J. Liu, *J. Phys. Chem. B*, **109**, 13406 (2005).
6. S. J. Tans, A. R. M. Verschueren, and C. Dekker, *Nature (London)*, **393**, 49 (1998).
7. A. Bezryadin, A. R. M. Verschueren, S. J. Tans, and C. Dekker, *Phys. Rev. Lett.*, **80**, 4036 (1998).
8. N. R. Franklin, Q. Wang, T. W. Tombler, A. Javey, M. Shim, and H. Dai, *Appl. Phys. Lett.*, **81**, 913 (2002).
9. M. A. Guillorn, M. D. Haile, V. J. Merkulov, M. L. Simpson, G. Y. Eres, H. Cui, A. A. Puretzky, and D. B. Geohegan, *Appl. Phys. Lett.*, **81**, 2860 (2002).
10. K. A. Watson, S. Ghose, D. M. Delozier, J. G. Smith, and J. W. Connell, *Polymer*, **46**, 2076 (2005).
11. B. J. Landi, R. P. Raffaelle, S. L. Castro, and S. G. Bailey, *Prog. Photovoltaics*, **13**, 165 (2005).
12. H. Pan, Y. P. Feng, and J. Y. Lin, *Phys. Rev. B*, **70**, 245425 (2004).
13. W. Zhao, C. Song, and P. E. J. Pehrsson, *J. Am. Chem. Soc.*, **124**, 12418 (2002).
14. M. Zheng and B. A. Diner, *J. Am. Chem. Soc.*, **126**, 15490 (2004).
15. Y. Cui, Q. Wei, H. Park, and C. M. Lieber, *Science*, **293**, 1289 (2001).
16. G. Dukovic, B. E. White, Z. Zhou, F. Wang, S. Jockusch, M. L. Steigerwald, T. F. Heinz, R. A. Friesner, N. J. Turro, and L. E. Brus, *J. Am. Chem. Soc.*, **126**, 15269 (2004).
17. T. Hertel, R. E. Walkup, and P. Avouris, *Phys. Rev. B*, **58**, 13870 (1998).
18. Q. Ngo, D. Petranovic, S. Krishnan, A. M. Cassell, Q. Ye, J. Li, M. Meyyappan, and C. Y. Yang, *IEEE Trans. Nanotechnol.*, **3**, 311 (2004).
19. G. H. Bolt, *J. Phys. Chem.*, **61**, 1166 (1957).